

## **Production of High Energy Ions Near an Ion Thruster Discharge Hollow Cathode**

I. Katz, I.G. Mikellides, D.M. Goebel, K. K. Jameson, R. Wirz, and James E. Polk  
Jet Propulsion Laboratory, California Institute of Technology,  
Pasadena, CA

### **Abstract**

Several researchers have measured ions leaving ion thruster discharge chambers with energies far greater than measured discharge chamber potentials. Presented in this paper is a new mechanism for the generation of high energy ions and a comparison with measured ion spectra. The source of high energy ions has been a puzzle because they not only have energies in excess of measured steady state potentials, but as reported by Goebel et. al. [1], their flux is independent of the amplitude of time dependent plasma fluctuations. The mechanism relies on the charge exchange neutralization of xenon ions accelerated radially into the potential trough in front of the discharge cathode. Previous researchers [2] have identified the importance of charge exchange in this region as a mechanism for protecting discharge cathode surfaces from ion bombardment. This paper is the first to identify how charge exchange in this region can lead to ion energy enhancement.

### **Introduction**

Several researchers have measured ions leaving ion thruster discharge chambers with energies far greater than measured discharge chamber potentials. Presented in this paper is a new mechanism for the generation of high energy ions and a comparison with measured ion spectra. The source of high energy ions has been a puzzle because they not only have energies in excess of measured steady state potentials, but as reported by Goebel et. al. [1], their flux is independent of the amplitude of time dependent plasma fluctuations. The mechanism relies on the charge exchange neutralization of xenon ions accelerated radially into the potential trough in front of the discharge cathode. Previous researchers [2] have identified the importance of charge exchange in this region as a mechanism for protecting discharge cathode surfaces from ion bombardment. This paper is the first to identify how charge exchange in this region can lead to ion energy enhancement. The xenon neutrals produced through charge exchange maintain their kinetic energy as they transit the potential trough. If they are subsequently ionized elsewhere in the discharge chamber, they then have both their initial kinetic energy and the potential energy of the plasma where they are ionized. A numerical simulation calculates the magnitude of the high energy ion fluxes. These calculated fluxes are compared with both radial and axial measurements of ion spectra. The mechanism successfully reproduces the observed large fluxes of high energy ions emanating radially from the discharge cathode region, and the paucity of high energy ions in the axial direction. The proposed mechanism is very similar to the mechanism proposed previously by King & Gallimore [3] to explain high energy ions observed in Hall thruster plumes.

## Background

Over the past decades, several researchers have reported measurements of energetic ions emanating from the vicinity of the orifice in high current hollow cathodes.[4-9] Some of these researchers have measured ions with kinetic energy more than double the applied discharge voltage. Various ion acceleration mechanisms have been proposed, including potential hills and ion acoustic instabilities. However, no direct measurements have been reported of potentials high enough to account for the ion energies.

In this paper, we focus on a single hollow cathode operating condition, similar to conditions found near the discharge hollow cathode in the NSTAR thruster operating at full power. The cathode was operated with an applied magnetic field similar to that in NSTAR. Using techniques previously reported [10], very high resolution measurements have been made of the potential structure in the vicinity of the hollow cathode keeper orifice. Ion energy distributions were measured both radially and axially downstream of the hollow cathode using a retarding potential analyzer.

The hollow cathode discharge was operated at 26 volts. The maximum potential measured, including fluctuations was 46 volts [1]. While the axial RPA measured essentially no ions with energies exceeding the measured potentials, the RPA positioned radially from the cathode keeper orifice, measured a substantial flux of ions with energies greater than the peak potentials observed in plasma.

## Experimental Measurements

### Experimental setup

The experiments are conducted in the cathode facility at JPL. The facility has been extensively used in previous experiments where several measured plasma properties have been reported. [10] Figure 1 is a schematic drawing showing the facility, specifically showing the cathode relative to the anode, the RPA and the radially scanning emissive probe.

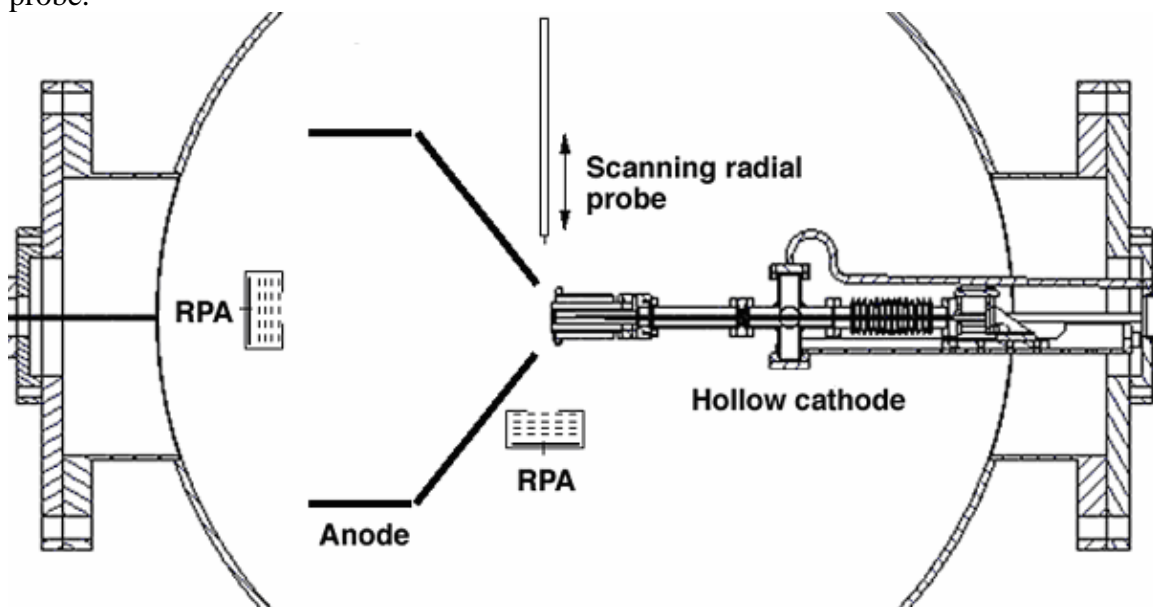


Figure 1. Schematic drawing of the cathode relative to the anode, RPA, and the radially scanning emissive probe.

The retarding potential analyzer is a four-grid arrangement, where the first grid in contact with the plasma floats, the second grid is biased to repel electrons, and only the ions with energy greater than potential applied to the dual-discriminator grid can pass through and reach the collector. The same RPA is positioned on axis and radially to measure the ion energy distribution function.

The radially scanning emissive probe uses a pneumatic plunger and is mounted to a Huntington X-Y manipulator outside the vacuum system to provide positioning relative to the keeper exit point. . The radial probe has a linear throw of 3 cm, at one meter per second, and is aligned by a slide-guide internal to the vacuum system to obtain a position resolution of 0.25 mm. The probe tip is a 0.127 mm diameter tungsten hair-pin wire feed through two side-by-side 0.5 mm diameter alumina tubes. A floating 5 amp power supply provides the current to heat the tungsten wire electrode to emit electrons.. The probe signal fed to a high impedance, high frequency circuit and a buffer amplifier to detect any oscillations present in the signal. For the complete experimental diagnostic tools used for comparison in the paper see Reference 10.

## **Results**

Ion energy spectra measured using a retarding potential analyzer (RPA) positioned radially and axially with respect to the hollow cathode orifice are shown in Figure 3. Time dependent radial potential distribution from reference 1 measured just down stream of the cathode keeper is shown in Figure 3.

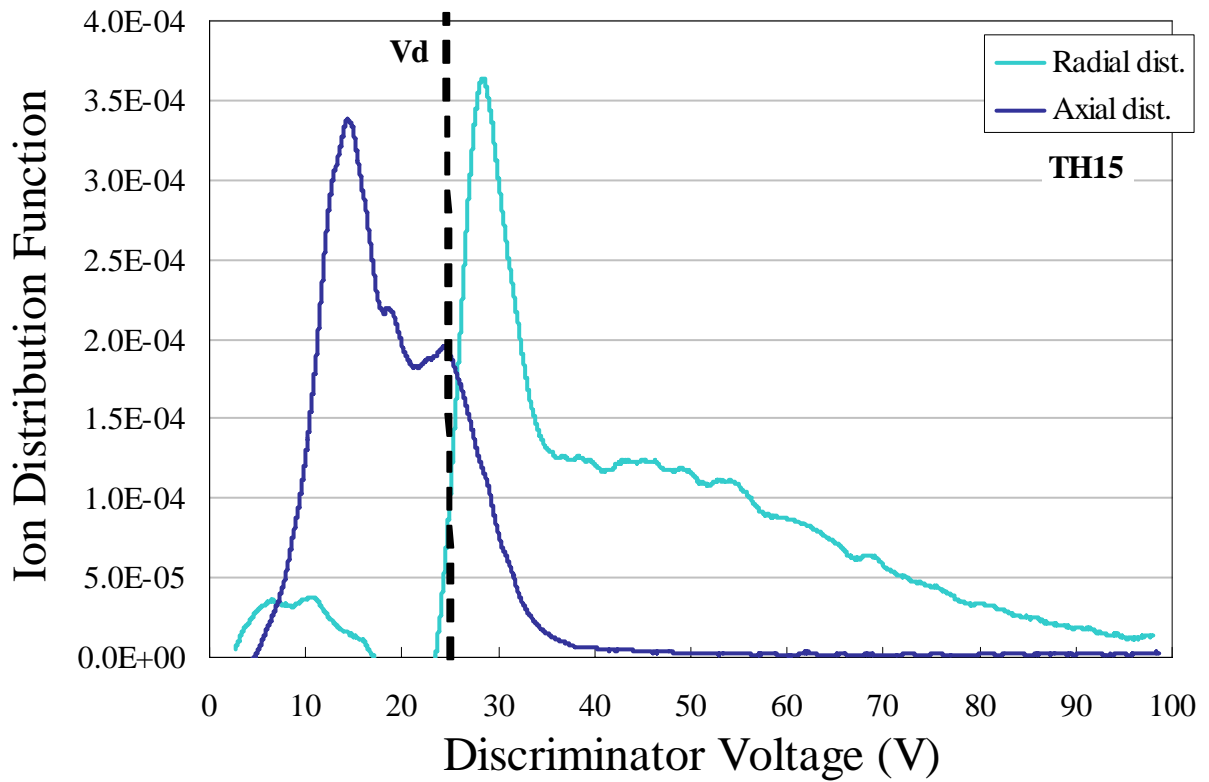


Figure 2. Measured distribution of ion energies for the RPA positioned radially and axially downstream of the cathode keeper orifice.

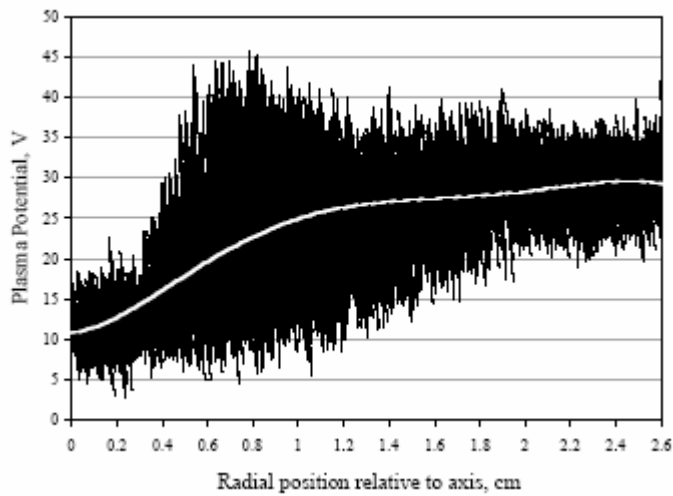


Figure 3 Plasma potential s function of radius from the axis showing large amplitude oscillations in the frequency range of 50 to 500 kHz (Ref 1)

**Proposed mechanism**

Immediately downstream of the discharge cathode keeper, the radial plasma potential profile has a substantial dip on axis. Ions generated on the edges of the potential dip are accelerated towards the centerline. The neutral gas density, which is dominated by un-ionized gas coming out of the hollow cathode, also peaks on axis. Near the cathode, the neutral gas density is high enough that a substantial fraction of ions are neutralized by resonant charge exchange with gas atoms before making it across the potential dip. Since they are now neutral, the Xenon atoms don't lose the kinetic energy they gained as ion falling into the dip as they pass through the other side of the potential dip. However, as they continue to drift radially, some of the atoms are ionized, either by charge exchange or collisions with electrons, and again are influenced the electric fields. By the time these ions reach the Retarding Potential Analyzer, they have their original thermal energy, the energy they gained falling down the dip, plus the energy from the plasma potential where they were re-ionized. This process is shown schematically in Figure 4. The changes in a ions kinetic energy is shown in Figure 5. The measured high energies comes because the when neutral, the xenon atom is not retarded by the potential rise, but immediately gains the potential energy.

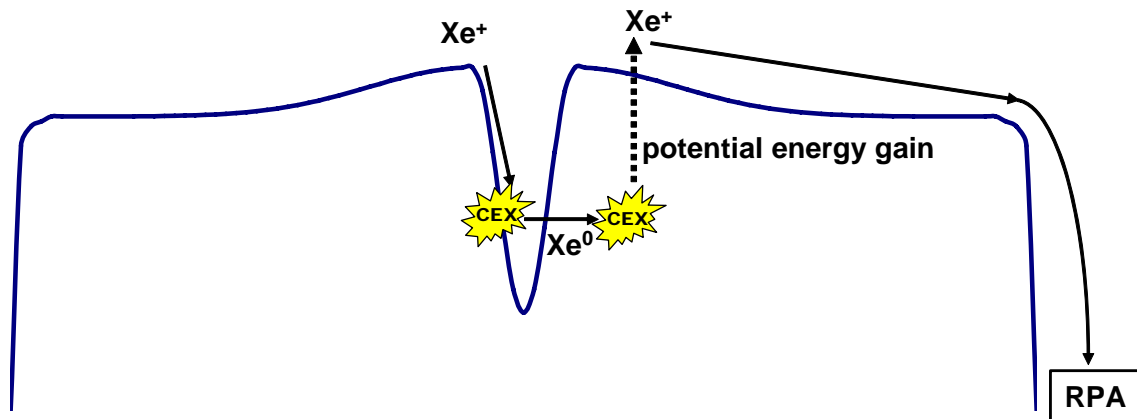


Figure 4. Xenon ions gain energy falling down potential well, are charge exchanged, travel past the potential rise without losing energy, and regain their charge in a high potential region.

This mechanism conserves energy between the two ions in the following manner. The original ion gains kinetic energy equal to the distance it falls down the central potential well. When it charge exchanges inside the well, the neutral left behind has only its own kinetic energy and the potential energy of the original ion in the well. When the second charge exchange occurs, the second ion's potential energy is given to the original xenon ion. The final state is two ions, one with high kinetic energy and high potential energy, the other has low kinetic energy and low potential energy. The sum of two ion kinetic and potential energies is the same before and after the two charge exchange collisions.

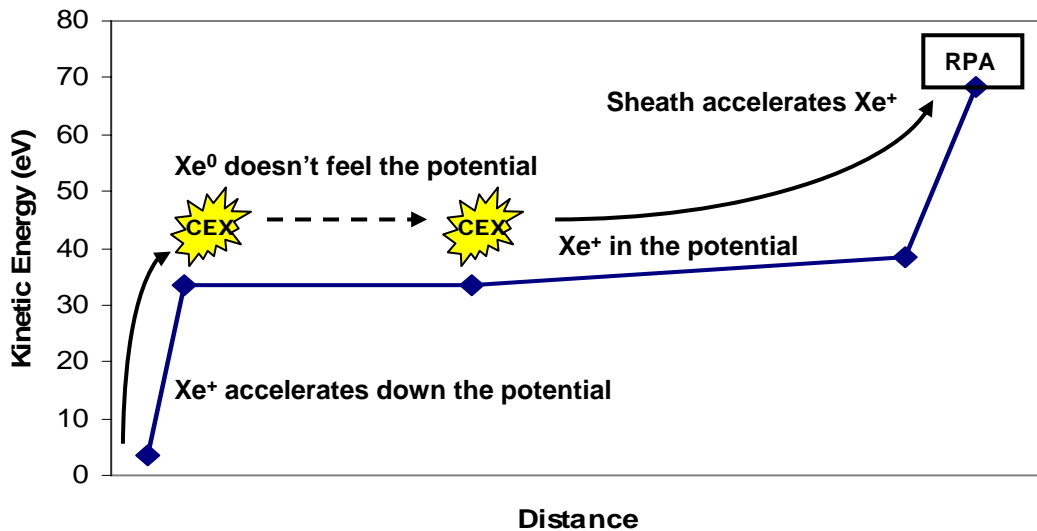


Figure 5. The Xenon ions gain most of their kinetic energy in the sheath and the potential well on axis.

### A Sample “Calculation”

To test the double charge exchange hypothesis, a rudimentary calculation was performed to estimate both the magnitude of the high energy ion current and the energy distribution function. The calculation was designed to test the reasonability of the hypothesis, not as a quantitative prediction of the ion distribution function: a self-consistent calculation of the ion and neutral gas densities, and electric potential is beyond the scope of the paper. The calculation performed assumes neutral and ion density profiles. The 2-D potential was calculated the using Ohm’s law and assuming classical plasma resistivity, in a grid, shown in Figure 6, that is conformal to the magnetic field. Because the electron motion near the cathode is strongly magnetically limited, the grid was chosen in order to accurately represent magnetic field effects on the potential. The cathode keeper orifice is located in the lower corner of the grid, and aimed along the Z-axis.

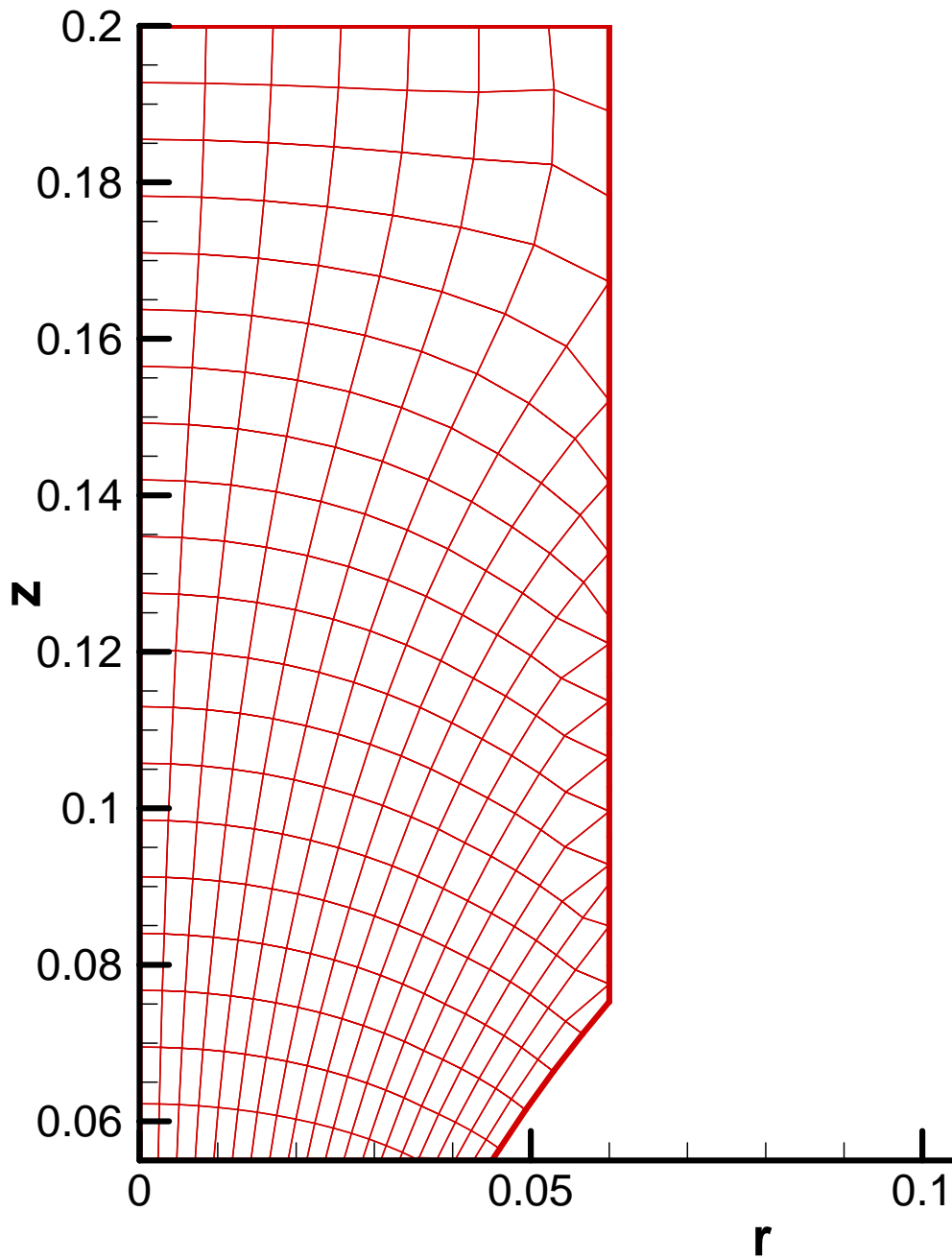


Figure 6 Computational grid where the grid lines near the axis are parallel and perpendicular to the magnetic field.

The ion density at the orifice was set to  $3 \times 10^{19} \text{ m}^{-3}$ , consistent with the measurements of Jameson, Goebel, and Watkins [10]. The ion density was assumed to fall as the inverse square of the distance from the orifice with a scale length of the keeper orifice radius. The neutral gas coming out of the keeper orifice was assumed to have a temperature of 800 K and a drift velocity equal to the one fifth the thermal velocity. The gas flux was 3.7 sccm. The magnetic field configuration was the model used in 2-D NSTAR discharge chamber simulations [11].

Electric potentials were calculated using Ohm's law with classical scattering frequencies and appropriate mobilities parallel and perpendicular to the magnetic field.

$$\mathbf{j} = \sigma \mathbf{E} + \sigma \frac{\nabla(nT_e)}{n}$$

$$\sigma_{\parallel} = \frac{ne^2}{m_e(\nu_{en} + \nu_{ei})}$$

$$\sigma_{\perp} = \frac{\sigma_{\parallel}}{1 + \Omega^2}$$

$$\Omega \equiv \frac{\omega_{ce}}{\nu_{en} + \nu_{ei}}$$

$$\omega_{ce} = \frac{eB}{m_e}$$

$$\mathbf{E} \equiv -\nabla\phi$$

$$\nabla \cdot \mathbf{j} = -\nabla \cdot (\sigma \nabla \phi) + \nabla \cdot \left( \sigma \frac{\nabla(nT_e)}{n} \right)$$

Contributions to the current by ionization are ignored. The current continuity equation reduces to Poisson's equation with anisotropic resistivity. The potential at the keeper orifice was set to 12 V as reported by Jameson[10], and the outer potential boundaries were set to 29 volts, corresponding to the cold ion peak in the measured spectrum. This is about an electron temperature higher than the anode potential, a condition consistent with a stable discharge.

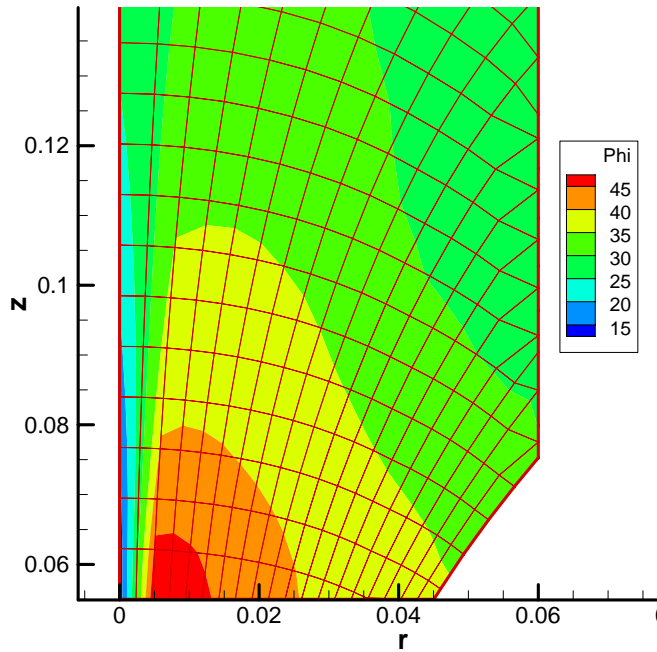


Figure 7 Calculated potentials near the cathode keeper orifice. Potentials in the vicinity of the keeper orifice are shown in Figure7. The potentials show the deep channel running along the axis, and a potential peak just outside the channel.

The potential peak arises from the pressure gradient term in Ohm's law, and coincides with the maximum ion density outside of the channel. While the calculated channel potentials appear similar to measurements, Figure 3, the current, calculated using classical resistivity, is much greater than measured. This is expected since the plasma inside the orifice channel is highly turbulent [12]. Turbulence reduces the plasma conductivity and in nature lowers the current for a fixed, applied voltage.

The trajectories of representative ions were calculated starting at the outer radial edge of the axial potential well and tracking them as they accelerated towards the axis. Since the electric fields in the well are primarily radial, the ions gained very little axial velocity; their motion was primarily radial. The probability of charge exchange and being converted into a fast neutral; was also calculated. The probability of an ion being charge exchanged into a neutral before it leaves the well ranges from almost half right near the keeper, down to a few percent a few centimeters downstream. The calculated total current of fast neutrals generated within 5 centimeters downstream of the keeper was 0.7 Amperes.

The probability of the fast neutrals being ionized was estimated as using the distance to the probe, 6.3 cm, and a background ion density of  $10^{18} \text{ m}^{-3}$ . The estimated probability of ionization was about 5%.

### **Comparison with measurement**

The magnitude of the calculated high energy ion current was compared with the ion current measured in the laboratory. The 3/16" disc probe was positioned at a radius of 6.3 cm from the axis, a few centimeters downstream of the keeper. The ion saturation current was 44  $\mu\text{A}$ . Based on the RPA spectrum (Figure 2), ions with energy greater than measured potentials accounted for about half the current, or 22  $\mu\text{A}$ . Assuming the fast ion current to be spread over a cylindrical area with a height of 10 cm, the calculated energetic ion current to the probe is 15  $\mu\text{A}$  with an uncertainty of at least 50%.

Using an assumed distribution of potential well depths shown in Figure 8, an ion spectrum was generated. The range potential well depths was estimated from the measured potentials (Figure 3) and approximated as a sine function for ease of integration. For any potential well depth, the spectrum calculation assumed uniform probability of charge exchange occurring at any energy. This approximation slightly under estimates the weight factor for higher energies, because the potential well is quadratic and the ions travel a longer distance with high velocities.

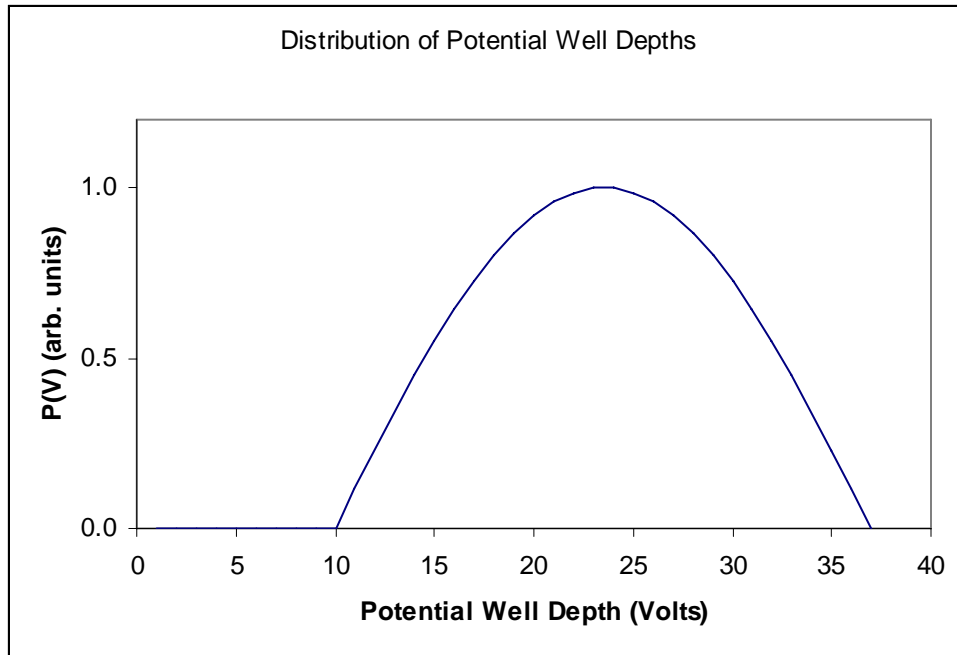


Figure 8 Distribution of axial potential well depths assumed in the ion spectrum calculation.

The calculated spectrum is shown in Figure 9. The primary, non-charge exchanged ion spectrum was estimated as a Maxwellian with a energy of 3.5 eV, the measured electron temperature. The high energy ion portion of the spectrum, while lower than the measurement, shows the same general features. The calculated spectrum has no ions above 95V, while the measured spectrum shows a few. It is expected these very high energy ions started out as double ions when they entered the axial potential well, and picked up twice the kinetic energy prior to being neutralized by charge exchange. The double ion resonant charge exchange cross section is about 25% of the single ion cross section.

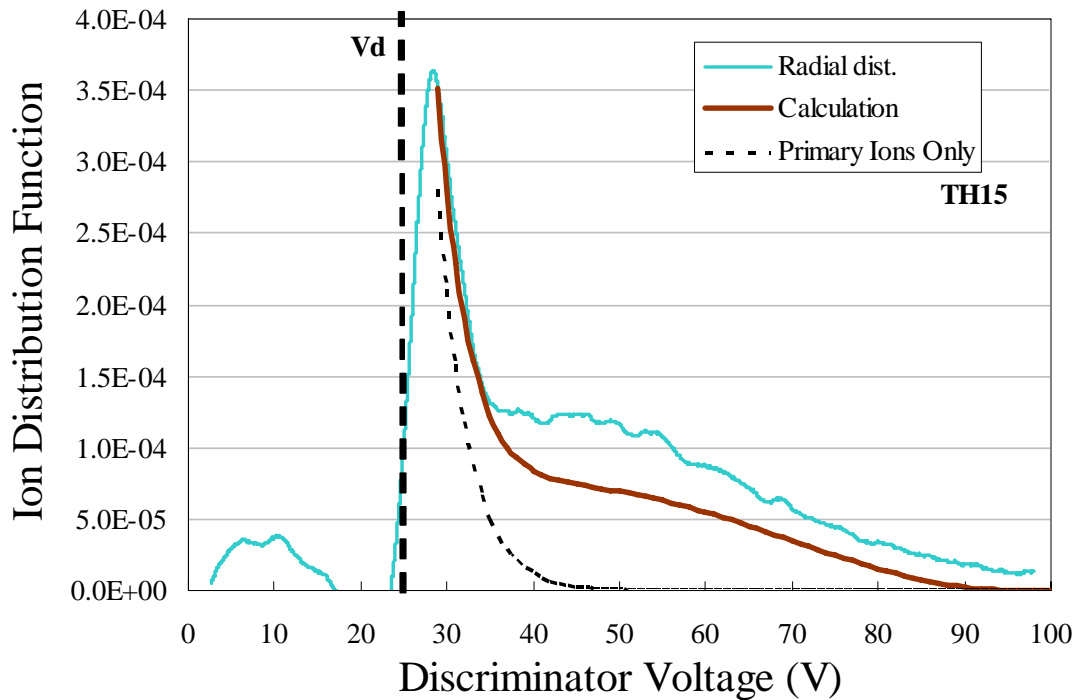


Figure 9 Calculated ion energy distribution compared with measurement.

### Discussion

The probability of charge exchange near the discharge cathode keeper orifice was previously identified by Rovey, Gallimore, and Herman [Ref 2] as high enough to protect the orifice from sputter erosion. It was shown that ions accelerated axially would undergo charge exchange before entering the keeper orifice sheath. While the previous work focused on axially accelerated ions, the present paper has shown the importance of charge exchange collisions on radially accelerated ions.

The mechanism presented above requires that an observed high energy ion have experienced two charge exchange collisions. However, because the resonant charge exchange cross section for xenon is so large, about  $70 \text{ \AA}^2$  [15], the probability of two charge exchange collisions, while small, is still large enough to account for the observed high energy currents. While previous studies showed how measured high energy ions resulted from charge exchange changing the charge to mass ratio on multiply charged ions [3], in this study ions temporarily neutralized ions gained potential energy without losing their kinetic energy, because while neutralized, their motion was unaffected by the electric field. Energy is conserved, although it is redistributed among the original ion and two other xenon atoms.

Finally, while the calculations here are intended to support the hypothesis, they are not the self-consistent plasma models needed to predict thruster hollow cathode life and performance, such as those being developed by Mikellides [12]. Furthermore, these ions with their high radial velocities are not the source of cathode keeper erosion.

## Acknowledgments

The research described in this paper was carried out by the Jet Propulsion Laboratory, California Institute of Technology, under a contract with the National Aeronautics and Space Administration.

1. Dan M. Goebel, Kristina Jameson, Ira Katz, Ioannis G. Mikellides, "Energetic Ion Production and Keeper Erosion in Hollow Cathode Discharges" IEPC-2005-266
2. Joshua L. Rovey, Alec D. Gallimore, and Daniel A. Herman, "Potential Structure and Propellant Flow Rate Theory for Ion Thruster Discharge Cathode Erosion", IEPC-2005-022
3. Lyon B. King and Alec D. Gallimore, "Ion-Energy Diagnostics in the Plasma Exhaust Plume of a Hall Thruster", *J. Propulsion & Power*, Vol. 16, No. 5, September–October 2000
4. V.J. Friedly and P.J. Wilbur, "High current hollow cathode phenomena", *J. Propulsion and Power*, **8**, 635 (1992).
5. I. Kameyama and P. Wilbur, "Measurement of ions from high current hollow cathodes using electrostatic energy analyzer", *J. Propulsion and Power*, **16**, 529 (2000).
6. G. Williams, et al., "Laser induced fluorescence characterization of ions emitted from hollow cathodes", *IEEE T-PS*, **28**, 1664 (2000).
7. J. Foster and M. Patterson, "Downstream ion energy distributions in a hollow cathode ring cusp discharge", *J. Propulsion and Power*, **21**, 144 (2005).
8. C. Farnell and J. Williams, "Characteristics of energetic ions from hollow cathodes", IEPC Paper 03-072, 28<sup>th</sup> International Electric Propulsion Conference, Toulouse, France, March 17-21, 2003.
9. C. Farnell and J. Williams, "Measurements of ion energy distributions produced within a NSTASR discharge chamber", AIAA Paper 2004-3432, 40th Joint Propulsion Conference, Ft. Lauderdale, FL, July 11-14, 2004.
10. K. Jameson, D.M. Goebel, R. Watkins, "Hollow Cathode and Thruster Discharge Chamber Plasma Measurements Using High-Speed Scanning Probes", IEPC-2005-269
11. R. Wirz, I. Katz, "Plasma Processes of DC Ion Thruster Discharge Chambers, 41st AIAA/ASME/SAE/ASEE Joint Propulsion Conference, Tucson, AZ, July 10-13, 2005", AIAA-2005-3690
12. I. G. Mikellides - cathode paper- JPC 2006
13. D.M. Goebel, K. Jameson, R. Watkins, I. Katz, "Hollow Cathode and Keeper-Region Plasma Measurements Using Ultra-Fast Miniature Scanning Probes", AIAA Paper #2004-3430, 40<sup>th</sup> Joint Propulsion Conference, Ft. Lauderdale, FL, July 11-14, 2004.
14. K. Jameson, D.M. Goebel, R. Watkins, "Hollow Cathode and Keeper-Region Plasma Measurements", AIAA Paper #2005-3667, 41<sup>th</sup> Joint Propulsion Conference, Tuscan, AZ, July 10-13, 2005.
15. Miller, J. S., Pullins, S. H., Levandier, D. J., Chiu Y., and Dressler, R. A., "Xenon Charge Exchange Cross Sections for Electrostatic Thruster Models," *Journal of Applied Physics*, Vol. 91, No. 3, 1 February 2002, pp. 984-991

